ELSEVIER

Journal of Hazardous Materials 55 (1997) 239–262

JOURNAL OF HAZARDOUS MATERIALS

Effects of conductive fractures during in-situ electroosmosis

Larry C. Murdoch [*,1], Jiann-Long Chen

Center for Geoenvironmental Science and Technology, Department of Civil and Environmental Engineering, University of Cincinnati, 1275 Section Road, Cincinnati, OH 45237, USA

Abstract

Hydraulic fracturing methods have been used to create horizontal disk-shaped fractures filled with sand to improve the discharge of wells in fine-grained formations, and we have evaluated the feasibility of creating similar features filled with electrically conductive graphite to be used as electrodes during electroosmotic remediation of contaminated soils. The approach was to create two flat-lying conductive fractures, one above the other, and maintain an electrical potential difference between them. Water was held at a constant level in wells accessing each fracture and flow was induced by electroosmosis. Theoretical analyses of this approach indicate that hydraulic gradients will cause water to flow radially away from a well accessing the anode-fracture. It will move vertically through the soil by electroosmosis until it reaches the cathode-fracture, where it will converge on a recovery well under hydraulic gradients. As a result the electrical conductivity of the filled fracture is critical to the creation of an electrical field, and the hydraulic conductivity of the fracture and electroosmotic conductivity of the soil are critical to electroosmosis.

Field tests were conducted using fractures filled with granular graphite that is both hydraulically and electrically conductive. Results show that relatively uniform electrical potential gradients of 10–40 $V\,m^{-1}$ can be created between the filled fractures, and those gradients are consistent with the results of theoretical analyses. Electroosmotic flow rates of roughly 0.5 $l\,h^{-1}$ were observed during field tests and are similar to theoretical predictions. The tests conducted thus far have been in uncontaminated ground, but the encouraging results suggest that this may be an important technique to use during electrokinetic decontamination of soil. © 1997 Elsevier Science B.V.

Keywords: Conductive fractures; Wells; Hydraulic gradients

* Corresponding author.

[1] Current address: Geological Science Dept., 340 Brackett Hall, Box 341908, Clemson University, Clemson, South Carolina, SC 29634, USA. Tel.: + 1 864 656 2597.

PII S0304-3894(97)00026-5

1. Introduction

Hydraulic fractures are created by injecting fluid into a well casing until the injection pressure exceeds some critical value and the soil or rock enveloping the casing cracks. A slurry formed from a stiff gel and a granular solid (e.g. sand, graphite, iron, porous ceramic, and sodium percarbonate have all been used) is injected into the fracture as it grows away from the casing. The solid granules prop open the fracture after injection and form a broad, thin layer in the subsurface. In overconsolidated soil, hydraulic fractures are typically flat-lying to gently dipping disks, roughly 0.5–1 cm thick and 5–10 m in diameter [1,2].

In most environmental applications, hydraulic fractures are filled with coarse-grained sand to provide high-permeability layers that increase fluid flow primarily by reducing the losses of hydraulic head in the vicinity of a well [1,2]. The discharge of liquids or vapors from wells can be increased by 1–2 orders of magnitude in many fine-grained formations [2]. This improved performance results from a change in the geometry of flow near the well, from sharply converging flow paths that result in head losses near conventional wells to nearly parallel flow paths normal to hydraulically conductive fractures.

Increasing the discharge of a well will improve the recovery of contaminants from the subsurface by advective processes. Effects related to adsorption, preferential flow, diffusion and other processes can result in mass transfer limitations that require a large number of pore volumes of fluid to be moved before soil is remediated using advection alone. One approach to address those limitations is to augment hydraulic advection with electrokinetics. In this process, a direct current is applied to the sediment to induce electroosmotic movement of water away from an anode and toward a cathode [3]. Rates of water flow by electroosmosis can be several orders of magnitude greater than by hydraulic flow in fine-grained sediments. Dissolved, neutral compounds can migrate with water flowing by electroosmosis, providing a possible mechanism to transport some organic compounds. Charged compounds, such as metal ions or colloids, will migrate toward the electrode with a charge opposite from the one that they carry [3,4]. Transport by electromigration may outpace movement by electroosmosis, or it may occur in situations where electroosmosis is inhibited.

On the basis of the results of laboratory tests [4–6] and limited field applications [7], electrokinetics appears to be a promising method of recovering ionic and water-soluble contaminants. However, the process is not without drawbacks. Field applications that use rod-like electrodes can suffer from large potential losses as the electrical field converges in the vicinity of the electrodes. Hydraulic fractures filled with electrically conductive material, such as graphite or metal, will reduce the potential losses and improve the performance of electrodes, just as hydraulically conductive fractures improve the performance of wells.

Electrochemical effects associated with pH changes at electrodes can cause minerals to precipitate in soil pores, markedly reducing permeability and inhibiting recovery. It may be possible to mitigate problems related to pH by circulating a buffering solution across the electrodes [7]. However, even if the electrodes can be buffered, the rate of migration by electrokinetics is slow enough in many soils to require electrode placement

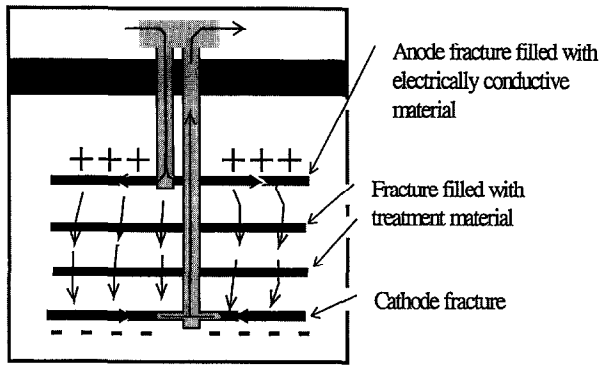

Fig. 1. Cross-section showing electroosmotic circulation of water between hydraulic fractures filled with conductive material such as graphite. Water flows through fractures filled with materials that can treat contaminants.

on a closely spaced grid in order to recover contaminants. An alternative approach that would address those limitations is to degrade contaminants in situ.

Our colleagues have developed a solid compound [8] that releases oxygen over several months and can be combined with a solid, slowly dissolving nutrient source to stimulate in-situ aerobic biodegradation. In addition, Gillham and Burris [9], among others, have shown that zero-valent metals, such as iron particles, will degrade a wide range of chlorinated organic compounds. It is feasible to inject those or other solid compounds into hydraulic fractures to create sheet-like layers capable of degrading contaminants in situ. Periodically reversing the polarity of the electric field will repeatedly pass contaminants through a degradation zone while limiting the development of high or low pH conditions in the vicinities of electrodes and reducing fouling of electrodes by precipitation. Combining electroosmosis with in-situ degradation is the essence of the so-called 'Lasagna' process (Fig. 1 [10]).

We have conducted theoretical analyses and field trials of water circulation associated with electroosmosis between two conductive hydraulic fractures; preliminary results of our work are described in the following pages. Basic principles of the process and theoretical analyses of idealized conditions are presented in Section 2, and essential details of recent field tests are given in Section 3.

2. Principles and theoretical analyses

Hydraulic fractures are heterogeneities that will change the fields of electrical and hydraulic potential. Material filling a fracture may differ from enveloping soil in either hydraulic conductivity K_h, electrical conductivity σ, or electroosmotic conductivity K_{eo}. Indeed, it is the very contrast in conductive properties between a filled fracture and the soil that will be exploited to enhance electroosmosis (EO).

Some effects related to the use of hydraulic fractures during electroosmosis can be anticipated by idealizing the fractures as conductive disks in a 2-D cylindrical coordinate system. The analysis will be used to predict fields of electrical and hydraulic potential,

as well as electroosmotic (EO) flux and total flow. Assumptions and methods of analysis are outlined in Appendix A.

Fractures created for field testing were 2.5–3.5 m in diameter, approximately 0.5 cm in average thickness, at depths of 1–3.5 m, and the currents applied were in the range of 20–40 A. Simulations were done for conditions within those ranges.

2.1. Electrical potential

The electrical potential field resulting from a typical configuration (Fig. 2) has nearly parallel isopotential lines between the fractures, and lines that curve sharply beyond the radial limit of the fractures. Accordingly, the gradient in electrical potential is roughly uniform between the fractures and decreases markedly beyond their radial extent. The potential decreases slightly along the radius of the fracture due to the finite conductivity of the graphite filling. Most of the fracture is at 80–90% of the applied potential, so the electrical potential gradient between the fractures available for electroosmosis is 60–80% of the voltage difference at the electrodes divided by the fracture spacing.

The current flux between the fractures in this example is between 0.70 and 0.85 $A\,m^{-2}$, with maximum values between the axes of the fractures and near their tips. A flux of 1.47 $A\,m^{-2}$ would occur if all the applied current stayed within the limits of the fracture (i.e. one-dimensional flow normal to the fractures). Thus, the region between the fractures supports a current flux of 50–60% of that expected for a one-dimensional idealization. A large flux occurs at the fracture tips because current converges on those points.

Electrical conductivity of the fractures, σ_{frx}, is the most important parameter affecting the distribution of the electrical field. In Fig. 2, a value of 200 $S\,m^{-1}$ was used because it is a conservative value for granular graphite used in the field tests. A variety of other grades of graphite and perhaps other materials are available to fill fractures, so we evaluated the effect of σ_{frx} on the resulting electrical field. The field was

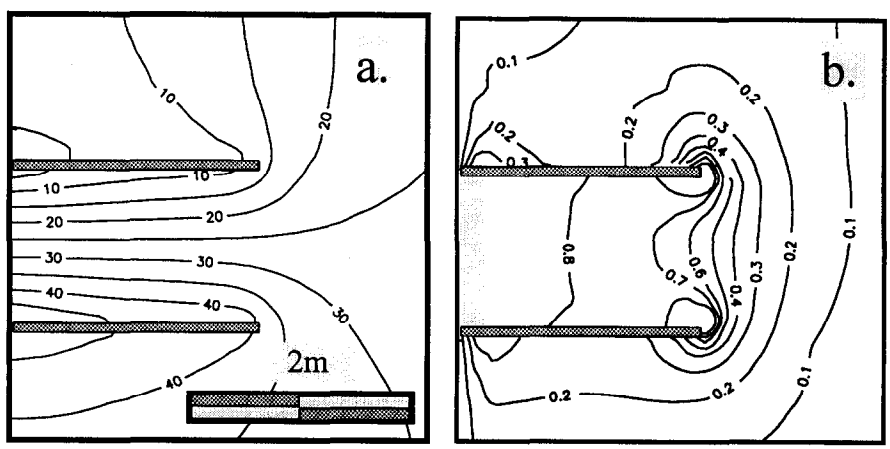

Fig. 2. Electrical potential (V) and current flux ($A\,m^{-2}$) in the vicinity of two electrically conductive disk-shaped fractures. Current: 30 A; σ_{soil}: 0.03 $S\,m^{-1}$; σ_{frx}: 200 $S\,m^{-1}$; thickness: 0.005 m; fracture depths 1.5 and 3 m.

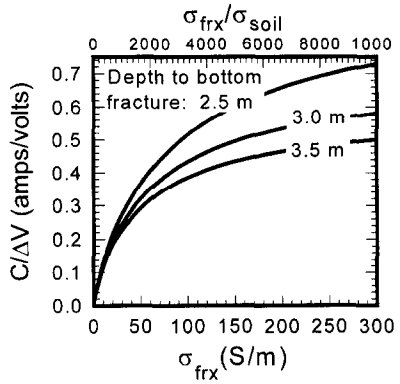

Fig. 3. Specific electrical current as a function of the conductivity and spacing of hydraulic fractures. σ_{soil}: $0.03\,S\,m^{-1}$.

characterized by the specific electrical current, which is the ratio of electrical current to applied potential difference between fractures (the inverse of the electrical resistance). This ratio is constant for applied currents over a practical range and serves as an indicator of the uniformity of the electrical field (the ratio increases as the field becomes more uniform between the fractures). Three fracture spacings were also evaluated, with the upper fracture at a depth of 1.5 m and the lower one at a depth of either 2.5, 3.0 or 3.5 m.

Specific current increases markedly with σ_{frx} for all spacings of fractures (Fig. 3). The results for low conductivity fractures are essentially those of a dipole, with the fracture contributing negligibly to the electrical field. The rate of increase of specific current diminishes as σ_{frx} exceeds approximately $150\,S\,m^{-1}$, or 5000 times σ_{soil} (Fig. 3). The specific current is approximately inversely proportional to fracture spacing, decreasing as the spacing increases.

The analysis in Fig. 3 indicates that σ_{frx} should be at least $150\,S\,m^{-1}$ for fractures that are 5 mm thick and for $\sigma_{soil} = 0.03\,S\,m^{-1}$. Similar results are obtained in more conductive soils if the ratio $\sigma_{frx} = \sigma_{soil} \geq 5000$ is preserved. Accordingly, where $\sigma_{soil} = 0.1\,S\,m^{-1}$ it follows that σ_{frx} should be $500\,S\,m^{-1}$ or greater. Those values can be achieved with commercially available granular graphite.

2.2. Electroosmotic flow

The flow of water in the vicinity of conductive fractures is driven by gradients in both electrical and hydraulic potential. Hydraulic potential gradients may result from externally applied conditions, such as an injection well, or they may result from heterogeneities or boundary effects accompanying electroosmosis, even when no external hydraulic gradients are imposed [11,12]. The general pattern of the hydraulic potential field depends on the depths and spacings of the fractures, the conductivities of the soil and fracture filling, and boundary conditions. As an example, we will assume that the configuration shown in Fig. 2 has far-field boundaries that are no flow, and that points at the origin of both the upper and lower fractures are held at a reference head of 0. These assumptions could be implemented in the field by covering the site with an

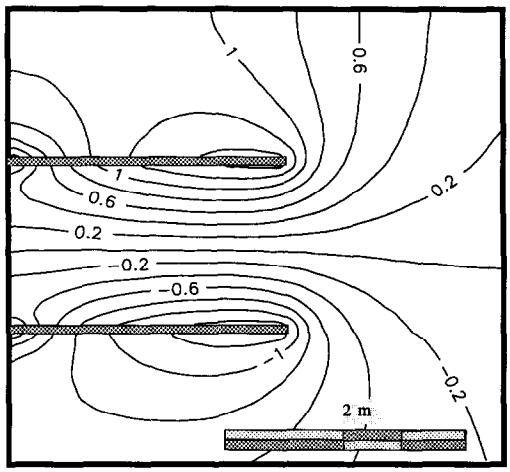

Fig. 4. Hydraulic head (m) in the vicinity of hydraulic fractures during electroosmosis. K_{hsoil}: 10^{-8} m s^{-1}; K_{hfrx}: 10^{-5} m s^{-1}. Other parameters as in Fig. 2.

insulating, impermeable layer, and by placing water-level control devices in wells accessing each fracture.

Those assumptions produce head gradients along the radius of the fractures with relatively high or low head near the tips of the upper and lower fractures, respectively (Fig. 4). Interestingly, the analysis indicates that water will flow parallel to a permeable fracture chiefly by hydraulic gradients, even though no hydraulic gradients are imposed. These hydraulic gradients result from the contrast in conductivities between the fracture and the soil.

The appearance of hydraulic gradients where none are imposed on a boundary is initially surprising. It results from non-zero values of β, which is tantamount to a fluid source, produced by spatial variations in conductivities according to eq. (A-4) (see Appendix). Similar hydraulic gradients are seen in electroosmotic column experiments where the outflow is restricted [11,12], or they are anticipated where chemical reactions change the conductivity of the soil [4].

Another consequence of this effect is the development of a hydraulic head gradient that opposes electroosmotic flux in soil between the fractures. The electroosmotic flux is always greater (at least for values typical of field conditions) than the hydraulic flux, but the backward-acting hydraulic flux serves to diminish the electroosmotic effect and thus to reduce the total flow rate.

The analyses indicate that a general scenario for electroosmosis between hydraulic fractures is as follows: water flows from a well accessing the anode-fracture driven primarily by hydraulic gradients; it then moves out of the fracture and through the soil under electrical gradients, and returns along the cathode-fracture under hydraulic gradients. It follows that as K_{hfrx} decreases, the hydraulic flow along the fracture is diminished and so is the total flow through the system (Fig. 5). The total flow approaches some small value determined by the electroosmotic flow along the fracture

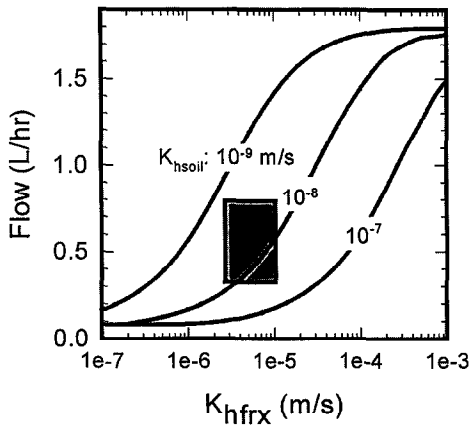

Fig. 5. Recovery from cathode well during electroosmosis, using configuration shown in Fig. 2, as functions of hydraulic conductivities of the fractures and the soil. K_{eo}: $5\times10^{-10}\,m^2(Vs)^{-1}$. The K_{hfrx} and K_{hsoil} occur within the boxed region during field tests.

as K_{hfrx} becomes small, whereas it approaches some maximal value, which is slightly greater than the 1-dimensional electroosmotic flow between the fractures as K_{hfrx} becomes large (Fig. 5).

The hydraulic conductivity of the soil also affects the total flow rate, with the flow due to electroosmosis decreasing as K_{hsoil} increases (Fig. 5). The flow rate can decrease by as much as $0.5\,l\,h^{-1}$, for example, as K_{hsoil} increases by an order of magnitude according to Fig. 5. This occurs because the backward-acting hydraulic flux induced by electroosmosis increases as the soil becomes more permeable. This has practical implications because it places a limit on the types of soil where electroosmosis will be useful using the configuration analyzed here. For example, an electroosmotic flow of roughly $1\,l\,h^{-1}$ appears feasible according to Fig. 5, but this same flow rate could be achieved with 1 m of differential hydraulic head between permeable fractures with a 2.5 m radius embedded in material where $K_{hsoil} = 5\times10^{-7}\,m\,s^{-1}$, roughly the conductivity of very fine sand or silt [13]. The value of K_{hsoil} where electroosmotic flow can be dwarfed by an imposed hydraulic flow will change somewhat by modifying either the applied electrical or the hydraulic potential relative to the values given above. But there are practical limits to the ceilings of both potentials, so we should expect that the configuration described above will significantly increase fluid flow by electroosmosis only in clayey silts to clays where K_{hsoil} is markedly less than $5\times10^{-7}\,m\,s^{-1}$.

3. Field studies

Graphite-filled hydraulic fractures have been used during in-situ electroosmosis at two sites near Cincinnati, Ohio. Preliminary tests of electrical potential distribution were conducted at the USEPA Center Hill Facility, Cincinnati, and more detailed tests of

water movement were conducted at a site in eastern Clermont county, approximately 30 miles east of Cincinnati. The latter site is owned by Browning and Ferris Industries and is managed by the Ohio Environmental Research and Education Center (OEREC).

3.1. Site conditions

Both sites were explored with borings and soil pits to evaluate conditions prior to and during testing. The Center Hill site is a flat-lying, grassy area underlain by at least 3 m of stiff to hard, orange-brown to brown, silty clay glacial drift. The soil is relatively uniform in the depth range of 1.5–3 m, although it becomes increasingly resistant and rocky below 3 m.

The soils were moist but unsaturated during testing; no free water was observed in piezometers. Porosity was 38–45% and hydraulic conductivity ranged from 5×10^{-7} to 5×10^{-8} m s^{-1}. The electrical conductivity increased with depth, from 0.04 S m^{-1} at 1 m to 0.11 S m^{-1} at 1.8 m, and it averaged approximately 0.05 S m^{-1} over the depth interval containing fractures (1.9–2.7 m).

The area of the OEREC test site is a flat-lying field once used for agriculture but now vegetated with indigenous plants. The soils are typical of the Rossmoyne Series, a silty clay loam that forms on the Illinoian till plain [14]. Beneath the topsoil there are two basic stratigraphic units; a mottled, gray-brown silt to silty clay in the upper 1.8 m, and a hard, brown silty clay with common sand- to pebble-sized rock fragments that occurs below 2.2 m. A heavily mottled transition zone separates the upper and lower units. The two units have strikingly different properties, as summarized in Fig. 6.

Water occurs in the transition zone and upper unit with the piezometric surface ranging from 0.5 to 1.5 m depth. The lower unit produces little water, although it is saturated. Porosity is 35–40% in the upper unit, but it decreases sharply to 16–20% in the lower unit. As a result, the moisture content of the lower unit is markedly less (7–8 wt%) than the upper unit (17–20%), even though the lower unit is saturated. The saturated hydraulic conductivity of the upper unit is 2×10^{-8}–7×10^{-8} m s^{-1}, based on in-situ tests made using a constant-head borehole permeameter, and K_h of the lower unit at a depth of 2.5 m is approximately 1×10^{-9} m s^{-1}. Electrical conductivity decreases from roughly 0.1 S m^{-1} in the upper to between 0.02 and 0.09 S m^{-1} in the lower unit (Fig. 6).

3.2. Materials and methods

Hydraulic fractures created during this study typically contained 270 kg of granular graphite and were initiated at depths from 1.4 to 2.7 m. They were roughly flat-lying with an average thickness of 4–6 mm and maximum dimensions of 4.5–6 m.

At the Center Hill site, fractures were created at depths of 1.93 and 2.70 m and were nearly horizontal. The fractures were approximately 2.5 m in radius and were created from separate bores approximately 1 m apart. As a result, the outer limits of the upper fracture were slightly offset from those of the lower one.

Two sets of fractures, location A and location B, were tested at the OEREC site. Location A was explored in detail by hand-augering and it contained several dozen piezometers and electrodes, whereas exploration of location B was minimized to avoid

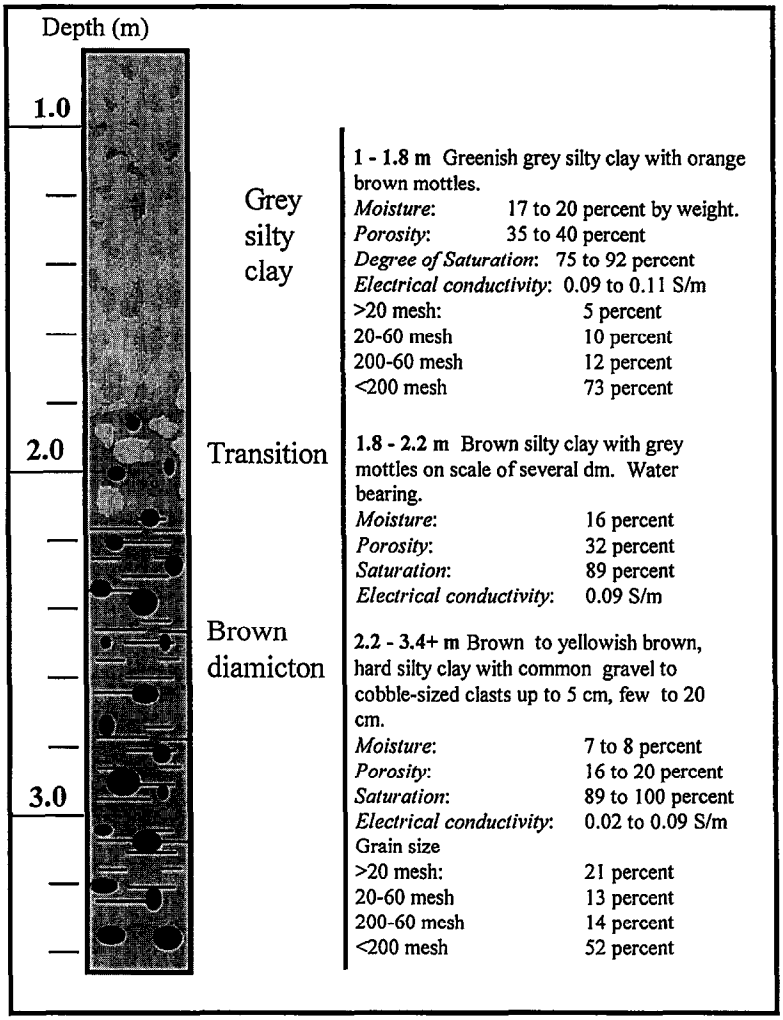

Fig. 6. Stratigraphic column and properties of soils at the OEREC site.

possible effects that the piezometers may have had on electroosmotic flow rate. The upper fracture at location A was initiated at 1.4 m depth and was bowl-shaped, climbing sharply near the injection point and then flattening out at roughly 1 m depth, but climbing to even shallower depths to the south (Fig. 7). The lower fracture at that location was initiated at a depth of 2.4 m, and available data indicate it is nearly horizontal.

Fractures at location B were filled with the same volume as those at location A, except that they were initiated approximately 1 m deeper, below the water table and entirely within the brown diamicton. Another important difference was that each graphite-filled fracture at location B had a sand-filled fracture created 0.2 m above or

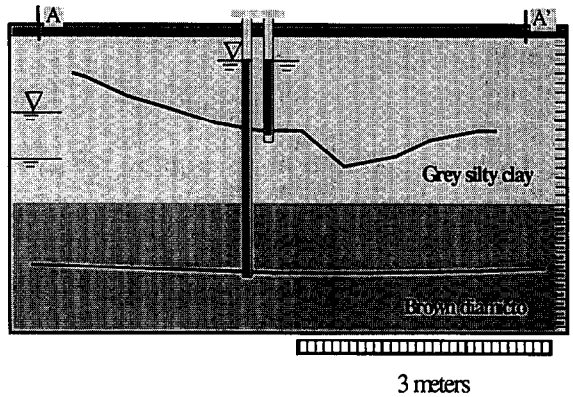

Fig. 7. Traces of hydraulic fractures and piezometric heads of wells accessing fractures at location A. Range of water levels in soil in vicinity of fracture is shown on left side.

below it in order to improve hydraulic flow. Accordingly, at location B the uppermost graphite-filled fracture was at 2.7 m depth and was underlain by a sand-filled fracture at 2.9 m, and the lowermost graphite-filled fracture was at 3.7 m and was overlain by a sand-filled fracture at 3.5 m.

3.2.1. Wells and piezometers

A variety of designs for completing power electrodes and wells were evaluated and the most satisfactory one was used at location B where the completion was constructed within a 4 inch PVC casing that was grouted in place. After the fractures were created, an assembly containing a water delivery tube and a power cable with an electrode (Fig. 8) was inserted in the well. Granular graphite was placed in the casing and the electrode was driven into the packing. The electrical resistance between the power electrode and the fracture itself decreased markedly as the force on the electrode increased. A packer

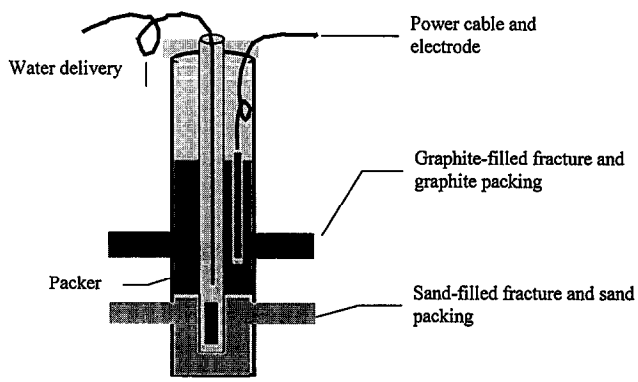

Fig. 8. Well completion used during test at location B.

separated that part of the well accessing the sand-filled fracture from the part accessing the graphite. This separation was used to isolate gases produced by hydrolysis from the circulating water.

Other well completions that were evaluated, such as those at Center Hill and OEREC location A, made use of 2 inch casings. Electrical contact between the fracture and the power electrode could readily be established using these completions, but in some cases the hydraulic conductivity around the well bore was apparently impaired. Increasing the size of the well bore markedly reduced problems related to well bore hydraulic conductivity.

A combination of piezometer and electrode was used to measure hydraulic head and electrical potential in the subsurface. It contained a PVC pipe with a filter pack of granular graphite. A stainless steel mesh covered the end of the pipe and allowed both hydraulic and electrical potential to be measured at the same location. The mesh-covered pipe was forced into the graphite to establish an electrical contact. Initial tests were conducted with piezometers open to the atmosphere, but they were later sealed after it was recognized that gas produced in the fractures could be escaping through the piezometers. The modification consisted of a tube that extended to the bottom of the piezometer pipe. One valve on the tube and another on the head space of the pipe allowed us to simultaneously measure the liquid level and the gas pressure.

Hydraulic heads varied naturally within the soil and were recorded using a datalogger attached to a transducer in a piezometer screened over 0.15 m and centered at 2.2 m depth, approximately the depth of the upper fracture. That piezometer was 7 m from location B and we assumed it characterized the far-field head as a function of time. Other piezometers screened nearby at different depths indicated that heads at any given time varied by several cm or more over the depth range 1–3.5 m. It was clear that vertical head gradients were present over the range of depths of the fractures, but only one piezometer was available to characterize the far-field head. We recognize that measurements from that piezometer will only approximate values of far-field head in the vicinity of fractures above or below 2.2 m.

3.2.2. Power supply

A solid-state, SCR-type dc power supply with an automatic closed-loop controller to maintain a constant current output was used to transform single-phase 230 V ac input to as much as 150 A dc at potentials up to 200 V. For safety reasons, potentials were limited by other circuitry to a maximum of 100 V dc with respect to a floating ground during field operations.

3.2.3. Properties of granular graphite

All the hydraulic fractures used during the field tests were filled with an electrical-grade graphite that was crushed and sieved to particles ranging from 0.1 to 4 mm in diameter (Table 1). Dry specific gravity of the bulk granular material is 1.0–1.1, porosity is 0.40–0.48 and void ratio is 0.92. The material used for this work is EC 181 7×100, from Graphite Sales, Chagrin Falls, OH. Electrical and hydraulic conductivity of the granular graphite were evaluated in detail because of their importance in electroosmosis.

Table 1
Grain-size distribution of granular graphite EC 181 7×100

Grain size(mm)	4.75	2.0	0.85	0.425	0.25	0.15	0.075
Average percent finer	100	81.5	44.6	21.4	9.6	4.6	0.9

3.2.3.1. Electrical conductivity. The electrical conductivity of bulk granular graphite was measured using an elongate rectangular cell (8 × 30 cm on its base) with a moveable, rigid plate on top and brass electrodes on each end. A layer of graphite approximately 1 cm thick was placed in the cell and the plate was loaded with a hydraulic cylinder. Conductivity was determined by passing several amps of electrical current through the electrodes and measuring the resulting voltage drop between stainless steel rods inserted through the plate. This procedure was repeated for wet or dry graphite under various confining pressures.

The electrical conductivity of the EC 181 7 × 100 graphite is 100–150 S m^{-1} under no load (Fig. 9), but it increases markedly as confining stress increases from 0 to 60 kPa (1 m depth of soil is roughly 18 kPa). The water content also affects conductivity, with saturated graphite 1.5–2 times more conductive than the dry material. At the depths of the field experiments, σ ranges from 400 to 1200 S m^{-1}, depending on confining stress and water content. A second-order regression fits the laboratory data well (Fig. 9), using the parameters in Table 2. Electrical conductivity under partially saturated conditions is unavailable, but it will be bounded by the data shown here.

3.2.3.2. Hydraulic conductivity. The saturated hydraulic conductivity of the granular graphite decreases slightly with increasing confining pressure. It is 10^{-5} m s^{-1} under no confining pressure, but decreases to 8.6×10^{-6} m s^{-1} under 40 kPa and to 6.0×10^{-6} m s^{-1} under 80 kPa of confining pressure in a flexible-wall permeameter.

The unsaturated hydraulic conductivity was approximated as a function of moisture tension using a parameter estimation scheme based on the moisture characteristic and described by van Genuchten [15]. To use this approach, the volumetric moisture content was determined as a function of moisture tension by step-wise desaturation using a

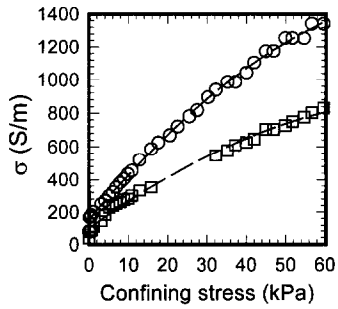

Fig. 9. Electrical conductivity of wet (circles) and dry (squares) EC 181 7×100 graphite as a function of confining stress. Regression lines used the parameters in Table 2.

Table 2
Regression equation for σ ($S\,m^{-1}$) of wet and dry granular graphite as a function of confining stress, s_c (kPa)

$\sigma = a_0 + a_1 s_c + a_2^2 s_c^2$

	Dry	Wet
a_0	101.1 ($S\,m^{-1}$)	155.5 ($S\,m^{-1}$)
a_1	17.57 ($S\,m\,kPa^{-1}$)	28.63 ($S\,m\,kPa^{-1}$)
a_2	−0.0971 ($S\,m\,kPa^{-2}$)	−0.144 ($S\,m\,kPa^{-2}$)
r^2	0.9910	0.9974

Buchner funnel. This test indicates that the granular graphite drains readily under a few cm of tension and approaches an apparent residual water content at roughly 60 cm tension (Fig. 10a).

The moisture tension relation was fitted to eq. 3 in van Genuchten [15] using the following parameters: $\theta_s = 0.41$, $\theta_r = 0.09$, $n = 2.7613$, $\alpha = 0.0960\,cm^{-1}$. The resulting curve is an excellent fit to the experimental data (Fig. 10a). Those parameters were used by van Genuchten ([15], eq. 9) along with measurements of K_{hsat} to produce the curve in Fig. 10b. The results indicate that the hydraulic conductivity drops precipitously with tension. Application of 60 cm of tension, for example, decreases the hydraulic conductivity by more than 5 orders of magnitude.

The curves shown in Fig. 10 were derived by assuming pore water tension was measured relative to atmospheric pressure. However, similar relations are expected if the gas pressure in the sample is greater than atmospheric and ΔP is taken as the difference

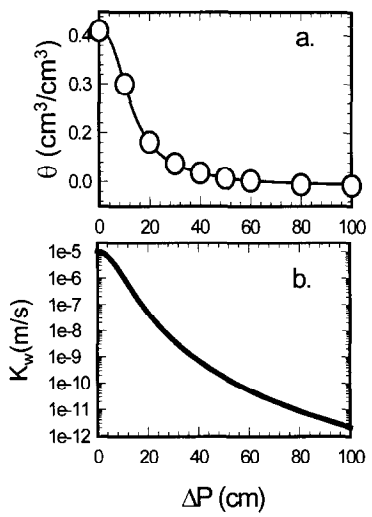

Fig. 10. (a) Volumetric water content of granular graphite as a function of difference between water pressure and gas pressure obtained experimentally (open circles) and based on van Genuchten ([15], eq. 3; solid line). (b) Hydraulic conductivity as a function of ΔP, from van Genuchten [15], eq. 9.

between the pore water and gas pressures. This will be relevant to the field study where gas was produced in the graphite-filled fractures.

3.3. Distribution of electrical potential

Tests of the distribution of electrical potential were conducted at the Center Hill site during summer, 1994. An array of 2 inch PVC pipes with stainless steel rivets along their length was installed at various radial distances to measure electrical potential. The tubes were pushed into tight-fitting bores so that the outside of the rivets firmly contacted the soil. An electrical wiper was lowered into the tube to measure the potential difference between a rivet and the cathode. Contact resistance between the wiper and the rivets was minor.

3.3.1. Field observations

Tests were conducted with the cathode at the upper and the anode at the lower fracture. Currents of 20–30 A were passed between the fractures, resulting in potential differences of 35–50 V. Throughout several weeks of testing the specific current remained essentially constant, ranging from 0.73 to 0.84 $A V^{-1}$. The surface area of the fractures was approximately 20 m^2, so the average current flux density was 1-1.5 $A m^{-2}$ (0.1–0.15 $mA cm^{-2}$) between the fractures, although this value could not be confirmed by direct measurement.

Electrical potential decreased as the cathode was approached from the ground surface. It reached a minimum of 3–5 V, or 10–15% of the applied potential, at the depth of the fracture and then increased markedly. The potential was greatest at the depth of the lower fracture, where it was 0.75–0.85 of the applied potential. This pattern was apparent within 2 m of the electrodes, and it resembled the pattern at $r = 2.6$ m although the maximum at the lower fracture was depressed at that point. We suspect that the monitoring tube at $r = 2.6$ m was within the radial extent of the upper but beyond the extent of the lower fracture (Fig. 11).

At radial distances beyond the extent of both fractures ($r = 3.5$ m), the potential distribution increased from the ground surface downward and varied only slightly from electrical ground (approximately 20 V). This contrasts with the region overlying the fractures where the shallow potential decreases with depth.

3.3.2. Modeling

Numerical methods described in Appendix A were used to evaluate the distribution of electrical potential by assuming the fractures were flat-lying disks 0.006 m thick at 1.93 and 2.75 m depth. The upper fracture was assumed to be 2.7 m in radius and the lower one 2.5 m. The conductivity of the material in the upper and lower fractures was assumed to be 1000 and 1200 $S m^{-1}$ respectively, which is consistent with Fig. 9. Electrical conductivity of the soil varied with depth from 0.02 to 0.05 $S m^{-1}$ according to field measurements, but in the model we assumed the soil was homogeneous and with a conductivity of 0.03 $S m^{-1}$.

The general pattern of electrical potential observed in the field can be predicted using the simplified assumptions outlined above (Fig. 11). Similar matches between field observations and theory are obtained at lower or higher applied currents, indicating that

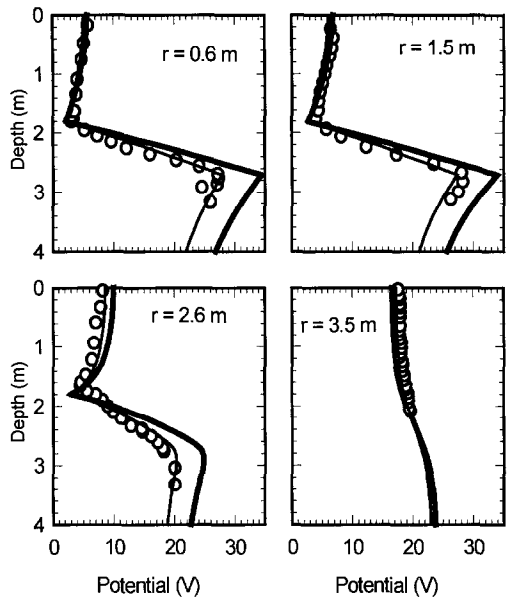

Fig. 11. Electrical potential as a function of depth at various distances from the power electrode. Points are field data. Heavy line is from theoretical analysis assuming homogeneous fractures; thin line is from analysis with contact resistance at lower fracture.

the electrical field in the vicinity of conductive hydraulic fractures can be predicted using simple analyses based on a few parameters (Fig. 11).

In detail, the model overpredicts the potential at the lower fracture by 5–8 V. The contact between the power cable and the fracture improved (based on measurements of specific current) as the power cable was forced into the graphite pack, probably as a result of a pressure-dependent contact resistance consistent with Fig. 9. We simulated a contact resistance by including a narrow 1.5 cm band of resistive material ($\sigma = 0.03\ \sigma_{frx}$) enveloping the anode power cable. Results of the simulation, including contact resistance, predict details of the potential profiles observed in the field (Fig. 11).

3.4. Fluid flow during electroosmosis

Three tests of electroosmotic flow between hydraulic fractures have been conducted thus far, with encouraging results coming from the last test at location B. The initial tests showed limited evidence for electroosmotic flow, probably because the well completion that was used resulted in low hydraulic conductivities when the power was turned on. This apparently occurred when gas resulting from hydrolysis occluded pores in the graphite packing enveloping the power electrode. Moreover, far-field piezometric heads were measured intermittently during the initial tests and we later found that those heads fluctuated by several dm, causing the flowrate at wells held at constant head to fluctuate. Consequently, it was only after modifying the well completion and recording the piezometric levels with a data logger that we could induce electroosmotic flow and account for the fluctuations caused by natural conditions.

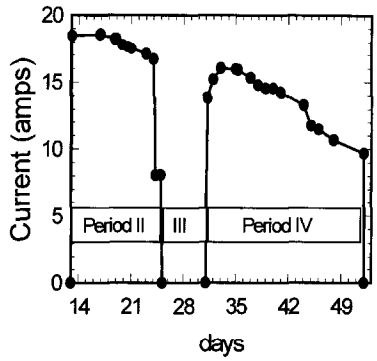

Fig. 12. Current as a function of time. Applied potential is 93 V.

The rate of injection or recovery from the well was controlled by water level sensors, which maintained the level in the well to within set points approximately 2 cm apart. The set points were placed at the depth of the piezometric surface at the start of the test. Injection or recovery rates were recorded every hour, the piezometric head was measured every 10 min, and then those values were averaged and recorded every hour using a data logger.

The test was initiated 25 January 1996 and consisted of five periods, with period I lasting for the first 2 weeks and representing initial baseline values (Fig. 12). Power was applied for nearly 2 weeks during period II and was shut off for a week during period III. The polarity of the electrodes was reversed and power applied again for 3 weeks during period IV. Flow was monitored for a week after power had been turned off at the end of the test.

Period I.	Day 0–13;	power off,	water measurements only
Period II.	Day 13–24;	power on,	lower fracture anode, upper cathode
Period III.	Day 24–31;	power off,	water measurements only
Period IV.	Day 32–52;	power on,	lower fracture cathode, upper anode
Period V.	Day 55–61;	power off,	water measurements only

The power supply was operated at maximum potential (approximately 93 V dc) throughout periods II and IV.

3.4.1. Voltage and current

The current that could be passed by the applied potential of 92 V was 18.5 A at the beginning of the test, but it decreased to nearly half that value (9.7 A) by the end of the test. This corresponds to specific currents of 0.2–0.1 $A V^{-1}$ (apparent resistance of 5–9.5 Ω). In contrast, similar configurations elsewhere at the OEREC site resulted in specific currents of 0.5–1 $A V^{-1}$, and the current was nearly constant during other tests of similar duration.

The power cable used for this test was terminated with an electrode of stainless steel, whereas graphite rods were used for all the other tests. The stainless steel was used because it is stronger than graphite and could be hammered into the graphite pack. However, the steadily decreasing current probably resulted from a steady degradation of the stainless steel anode during operation. As a result of these findings, steel or iron electrodes have been abandoned during our subsequent work in favor of rods formed from very fine-grained, relatively strong graphite.

3.4.2. Injection rate and piezometric head

The far-field piezometric head varied by 0.5 m and the flow rate required to maintain constant water level fluctuated over $4\,l\,h^{-1}$ in response to the variations during all periods of the test. Short-term changes in piezometric head followed precipitation events, which occurred regularly during the test. Likewise, short-term changes in flowrate accompanied the changes in piezometric head, with the rate of water recovery from the well increasing with a rise in piezometric head. It appears that flow rates at the wells are strongly influenced by piezometric head changes accompanying rainfall, an effect that occurs naturally and is unrelated to electroosmosis.

On the basis of theoretical analyses presented earlier (Fig. 5), we expect flow rates due to electroosmosis under the current conditions to be on the order of $0.5\,l\,h^{-1}$. Significantly greater flow rates occur naturally, although we should point out that those relatively large rates are short lived and may account for only minor displacements of fluid in the soil. Nevertheless, effects of electroosmosis on the flow rates cannot be detected when the data are plotted as a function of time, because the magnitude of naturally occurring flows is great enough to obscure expected electroosmotic effects.

Effects of electroosmosis are apparent, however, when the injection rate (negative values indicate recovery from the well) is plotted as a function of the far-field piezometric head (Fig. 13). At the upper fracture-electrode the data from the different periods occur in roughly linear bands. The slopes of the bands are similar, from 9 to $11\,l\,(h\,m)^{-1}$, but the y-intercepts are shifted by $1.0–1.4\,l\,h^{-1}$. The band with the greatest intercept occurs during period II when the upper fracture is the cathode, whereas the one with the least intercept occurs during period IV, when the upper fracture is the anode. The middle band contains data obtained during periods III and V (data from period I at the upper fracture are unusable due to equipment malfunction) when the power was off.

A similar behavior occurs at the lower electrode, although the slopes of the bands are flatter, $3–4\,l\,(h\,m)^{-1}$, and the linear relationships are more poorly defined than at the upper electrode. Nevertheless, the data band with the greatest intercept occurred when the lower electrode was the cathode, and the least intercept occurred when the lower electrode was the anode. Those intercepts differ by $1.0–1.6\,l\,h^{-1}$, just as at the upper electrode.

The field data indicate that the flow changed by $1.0–1.4\,l\,h^{-1}$ in response to changing the polarity of the electrodes, and the sign of this change is consistent with the effects expected by electroosmosis. Moreover, this effect appears to be relatively insensitive to piezometric head. We conclude that the flow due to electroosmosis is half the bandwidth cited above, or $0.5–0.7\,l\,h^{-1}$, and that flows of this magnitude can be achieved in either direction by changing polarity.

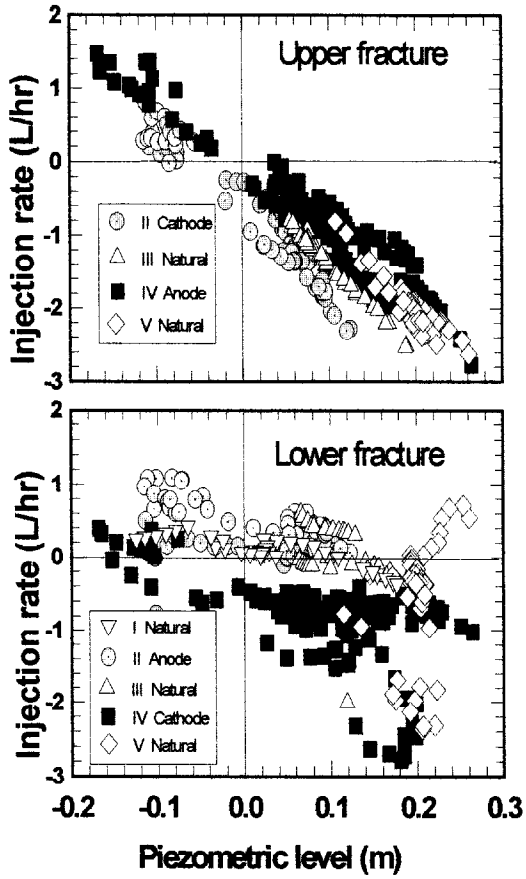

Fig. 13. Injection rate required to maintain constant head during electrosmosis test at location B with respect to piezometric level. The piezometric datum is between the set points at the upper well.

Theoretical analyses presented in Fig. 5 are based on conditions similar to this test, with the shaded box on that figure defining the observed range of hydraulic conductivities of soil and graphite. That analysis indicates that the steady flow rate between the fractures should be 0.3–0.8 $l\,h^{-1}$, depending on the actual conductivities at the site. The field observations validate this prediction.

The field data indicate that flow rate is approximately linearly related to far-field piezometric head; however, it is unrealistic to expect the relation to be exact. There will be a transient response, with the flow rate at the well depending not only on the instantaneous far-field piezometric head but also on how rapidly the head is changing. This effect is apparent in the field data, where flows during rapid changes differ from the flows during gradual changes in head. Moreover, the data in Fig. 13 are plotted with respect to far-field head at one location whose depth was similar to that of the upper fracture. Vertical head gradients are common at this site and would cause the far-field head at the depth of the lower fracture to differ from measurements made at shallower

depths. Those factors surely account for some of the scatter in the data shown in Fig. 13, and there are other related factors that could account for additional scatter. Detailed modeling of transient infiltration during electroosmosis could probably account for many of those factors, but such modeling is beyond the scope of our present effort and is unnecessary to support the conclusions regarding electroosmosis.

3.4.3. Temperature

Temperature in the vicinity of the fractures increases due to resistive heating accompanying the application of electric power. An array of thermocouples was used to measure temperature profiles during a test at OEREC location A that was similar in duration to the one described above but where the power was purposefully increased in several steps from 0.5 kW to 2 kW. Prior to turning on the power, temperatures in the soil ranged from 15°C at 3 m depth to 32°C a few cm from the ground surface, according to measurements 1 m from the electrode. During the first few weeks of the test, when modest power levels (0.5 kW) were used, temperature increased by 1–2°C per week, and the magnitude of change was relatively evenly distributed between the fractures. As the power level increased (to 2 kW), a maximum in the temperature profile developed at the upper fracture by day 47 (power turned on, day 14) and the soil warmed to 35°C by day 56 at the end of the test. The region cooled after the power had been turned off, but temperatures were still 10°C above ambient 14 days after this event (Fig. 14).

The soil cooled toward the edge of the fracture, and the general form of temperature profiles in Fig. 14 is representative of profiles elsewhere between the fractures. In the vicinities of the electrodes, however, temperatures increased abruptly when the power was applied and were significantly warmer than temperatures in the soil. At the anode, for example, the temperature increased to 60°C within 30 min while 0.5 kW was applied,

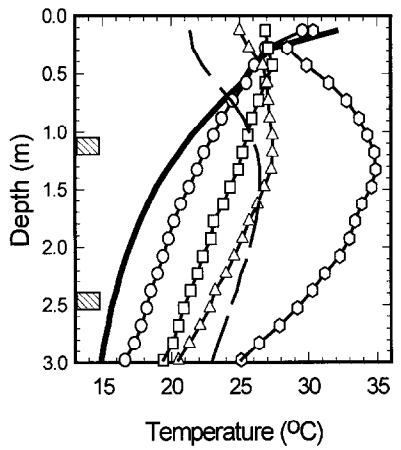

Fig. 14. Temperature as functions of depth and time 1 m from electrode. On day 14 the power was turned on, and it was turned off on day 56. Initial temperature on day 6 (heavy line), on day 20 (circles), day 31 (squares), day 47 (triangles), day 56 (hexagons), and on day 70 (dashed line). Gray boxes are depths of fractures.

and reached 100°C with 1 kW power. Boiling at the electrodes caused operational difficulties during early tests, presumably because granular graphite in the electrode became fluidized and the electrical contact between the fracture and the source cable was disrupted. We have operated the system described above while water boiled in the vicinity of the electrodes; however, this resulted in several equipment problems and we generally try to keep electrodes below boiling temperature.

3.5. Discussion

Tests at location B confirm that electroosmotic flow rates of the magnitude predicted by theoretical analyses can be achieved in the field, but data from tests at other locations showed that electroosmotic flow was either intermittent or absent altogether even though strong electrical potential gradients were created. Two key design changes in the well completion and the fracture itself probably resulted in the improved performance. At location B, the size of the well was increased and additional fractures filled with sand were created; both changes were intended to improve the hydraulic conductivity of the well and the fracture-electrode.

The theoretical analyses showed that a hydraulically conductive path from the well along the fracture is essential for electroosmotic flow to occur using the system described above. Hydraulic conductivities of graphite-filled fracture-electrodes completed with 2 inch wells and lacking the additional sand-filled fractures were measured using slug tests before the power was turned on, and these were similar to values obtained from laboratory tests using the granular graphite. Slug tests conducted while the power was on, however, indicate that the hydraulic conductivity of the fracture decreased by an order of magnitude or more. That reduction in K_{hfrx} will markedly diminish the electroosmotic flow rate according to Fig. 5.

We suspect that the decrease in hydraulic conductivity resulted from the formation of gas accompanying hydrolysis. Gas was observed bubbling vigorously at the power electrodes (even when temperatures were below boiling), and gas bubbles were observed in a few of the piezometers within 1 m of the electrodes. At other piezometers intersecting fracture-electrodes, we observed an increase in gas pressure in the piezometer head space, although at piezometers completed in soil the headspace pressure remained unchanged. The gases were presumably H_2 or CH_4 at the cathode and O_2 or CO_2 at the anode, although chemical analyses were not conducted.

Slight increases in gas pressure in the pores of the graphite can dramatically reduce the hydraulic conductivity. Gas pressure heads 20 cm greater than water will reduce the hydraulic conductivity by 2–3 orders of magnitude, according to Fig. 10. We suspect that this effect was responsible for inhibiting electroosmotic flow during the early tests.

The design utilized at location B is capable of inducing electroosmotic flow, but it is relatively complicated and would be cumbersome to implement on a widespread basis. Future implementations probably will make use of granular graphite with a narrow size distribution, lacking fine-grained material. Preliminary tests show that removing the fine graphite particles will reduce the electrical conductivity by a factor of two but increase the hydraulic conductivity by an order of magnitude or more. A reduction in electrical

conductivity of that magnitude will have negligible effects on the distribution of electrical potential, but an increase in hydraulic conductivity of that magnitude can have a marked effect on the electroosmotic flow rate.

4. Conclusions

It is feasible to create electrical fields and to induce flow by electroosmosis between two adjacent hydraulic fractures filled with electrically conductive material. Water moves radially from an access well along the anode-fracture by hydraulic flow, then moves through the soil by electroosmosis, and it returns by converging on an access well in the cathode-fracture by hydraulic flow. Accordingly, the electrical and hydraulic conductivities of the material filling the fracture must both be several orders of magnitude greater than those of the enveloping soil. Granular graphite was used to fill fractures during field tests conducted for this work.

Relatively uniform electrical potential gradients of 10–40 $V\,m^{-1}$ were created at two sites in the vicinity of Cincinnati, Ohio. Theoretical analyses indicate that the potential observed in the field can be predicted assuming a ratio $\sigma_{frx}/\sigma_{soil} = 5000$, which is readily achieved in most soils with commercially available graphite. The observations and analyses both indicate that vertical gradients in electrical potential can be estimated by

$$dV/dz = c\Delta V/b$$

where ΔV is the applied electrical potential difference between the fractures, b is the vertical spacing and c is a constant that ranges from 0.6 to 0.8 and depends on contact resistance at the electrode and other factors. The current flux density was approximately 0.5–1.5 $A\,m^{-2}$. Most of the region sandwiched between the electrode-fractures (20 m^3 of soil during the field tests) is subjected to that potential gradient and flux density.

Electroosmosis resulted in a flow rate of 0.5–0.7 $l\,h^{-1}$ during field tests using hydraulic fractures filled with graphite and sand. The direction of flow could be reversed by changing the polarity of the electrical field. Theoretical analyses predict that electroosmotic flow rates will be 0.3–0.8 $l\,h^{-1}$, and the field observations validate those predictions. The flow rate due to electroosmosis was less than that due to natural fluctuations of the water table, and could only be discerned when effects of the natural fluctuations were removed. Nevertheless, the natural fluctuations were short-lived responses to precipitation or diurnal temperature or barometric changes, and probably resulted in negligible displacements of water, whereas electroosmotic flow could be sustained at least for several weeks.

Circulation of water by electroosmosis is best suited to relatively tight soils with a hydraulic conductivity of 10^{-8} $m\,s^{-1}$ or less. Hydraulic flow may outpace electroosmotic flow in more permeable soils, although electromigration or electrophoresis may be useful remedial techniques in those materials. Hydraulic heads at wells accessing the fractures should be held at the same level as heads in the soil to highlight electroosmotic flow, but hydraulic gradients may be imposed to increase total flow rate without detrimentally affecting electroosmosis.

Gas formed by hydrolysis may cause partially saturated conditions that markedly reduce the hydraulic conductivity of the fractures and well bore, and this effect may reduce electroosmotic flow rates. Creating sand-filled fractures in the vicinity of the graphite-filled fracture-electrodes apparently increased hydraulic conductivity and reduced the detrimental effects of gas production. Recent preliminary tests indicate that using a well-sorted graphite may increase the hydraulic conductivity enough so that the sand-filled fractures are unnecessary.

The process described here should have several environmental applications. The electrical field produced between the hydraulic fractures is more uniform than that between vertical wells, so it may be useful during electroosmotic recovery of contaminants. Efforts are currently under way to extend this work by creating additional fractures filled with materials, such as zero-valent iron, that can degrade contaminants in soil between electrodes, thereby eliminating the need for recovery and above-ground treatment.

Acknowledgements

This work was funded by the USEPA under Cooperative Agreement CR-822677. We appreciate the help of Mike Roulier, Taras Bryndzia, and Wendy Davis-Hoover of the USEPA. We also appreciate the cooperation and assistance of Browning and Ferris Industries, who sponsor the Ohio Environmental Research and Education Center where much of the field work was conducted. The opinions and conclusions presented here are our own and are not necessarily those of the USEPA or Browning and Ferris Industries. No endorsement by the USEPA should be inferred. The work described here would have been impossible without the help of our colleagues Souhail Al-Abed, Phil Cluxton, Mark Kemper, Dave Kreuzmann, Bill Slack, and Steve Vesper.

Appendix A. Methods and assumptions used to analyze electroosmotic flow

Electroosmotic flow in the vicinity of two conductive disks will be analyzed as follows:

1. Determine the distribution of electrical potential.
2. Determine the distribution of fluid potential.
3. Determine fluxes from gradients of electrical and fluid potentials.

This approach tacitly assumes that the applied electrical potential results in fluid flow but that the resulting flow does not affect the electrical potential. This amounts to assuming that the streaming potential is negligible compared to electrical potentials applied during the process, which seems reasonable in light of the magnitudes of the applied potentials. The electrical potential distribution is determined in cylindrical coordinates according to

$$\frac{\partial}{\partial r}\left(\sigma\frac{\partial V}{\partial r}\right)+\frac{\sigma}{r}\frac{\partial V}{\partial r}+\frac{\partial}{\partial z}\left(\sigma\frac{\partial V}{\partial z}\right)+R_e=0 \tag{A-1}$$

where R_e is the electrical current applied or removed from the subsurface. The boundary conditions for the electrical potential distribution are

$$\begin{aligned} &V = V_0; \quad (\infty, z) \text{ and } (r, \infty) \\ &\frac{\partial V}{\partial z} = 0; \quad (r, 0) \\ &\frac{\partial V}{\partial r} = 0; \quad (0, z) \\ &R_e = \frac{\text{applied current}}{\text{volume of electrode}}; \quad \left(r \le r_e,\ z_{\text{upper}} + \frac{\delta}{2} \le z \le z_{\text{upper}} - \frac{\delta}{2}\right) \\ &R_e = -\frac{\text{applied current}}{\text{volume of electrode}}; \quad \left(r \le r_e,\ z_{\text{lower}} + \frac{\delta}{2} \le z \le z_{\text{lower}} - \frac{\delta}{2}\right) \end{aligned} \tag{A-2}$$

Fluid flow will be determined by assuming that the flux due to electroosmosis can be superimposed on the flux due to hydraulic flow as in eq. (A-1). From continuity and Darcy's Law we have

$$\frac{\partial}{\partial r}\left(K_h \frac{\partial \varphi}{\partial r}\right) + \frac{K_h}{r}\frac{\partial \varphi}{\partial r} + \frac{\partial}{\partial z}\left(K_h \frac{\partial \varphi}{\partial z}\right) + \beta = 0 \tag{A-3}$$

where β is a source term determined from the distributions of electrical potential and K_e:

$$\beta = \frac{\partial}{\partial r}\left(K_e \frac{\partial V}{\partial r}\right) + \frac{K_e}{r}\frac{\partial V}{\partial r} + \frac{\partial}{\partial z}\left(K_e \frac{\partial V}{\partial z}\right) \tag{A-4}$$

Boundary conditions for the fluid potential are

$$\begin{aligned} &\varphi = \varphi_0; \quad (\infty, z) \text{ and } (r, \infty) \\ &\frac{\partial \varphi}{\partial z} = 0; \quad (r, 0) \\ &\frac{\partial \varphi}{\partial r} = 0; \quad (r_e, z) \\ &\varphi = \varphi_{\text{upper}}; \quad (r_e, z_{\text{upper}}) \\ &\varphi = \varphi_{\text{lower}}; \quad (r_e, z_{\text{lower}}) \end{aligned} \tag{A-5}$$

The ground surface is assumed to be no-flow, which requires that the gradient in hydraulic potential is proportional to the gradient in electrical potential at the boundary. However, for the case analyzed here, no-flow boundaries for the fluid problem correspond to boundaries where the electrical potential gradients are zero, which results in the conditions given in eq. (A-5). We assume that the fluid potentials are maintained at constant values at the electrode wells.

The problem was solved by discretizing eq. (A-1) or eq. (A-3) in finite difference form and using Gauss–Seidel iteration and successive overrelaxation to solve the resulting simultaneous equations. A finite difference grid was used where the fractures

were idealized as disks that were somewhat thicker than the fractures in the field in order to limit the changes in cell size. Accordingly, the conductivities of the cells representing the fractures were adjusted to account for the difference between the width of the grid representing the fracture and the actual fracture in the field, using

$$K_{re} = \frac{K_f a + K_s(\delta z_f - a)}{\delta z_f} \tag{A-6a}$$

$$K_{ze} = \frac{\delta z_f}{\dfrac{K_f}{a} + \dfrac{K_s}{\delta z_f - a}} \tag{A-6b}$$

where a is the fracture aperture, δz_f is the thickness of the cell representing the fracture, K_f is the conductivity of the material filling the fracture, and K_s is the conductivity of the soil.

References

[1] Murdoch, L.C., A field test of hydraulic fracturing in glacial till, Proc. 15th Annual USEPA Research Symposium, Cincinnati, OH, 1990.
[2] Murdoch, L.C., Losonsky, G., Cluxton, P., Patterson, B., Klich, I. and Braswell, B., The feasibility of hydraulic fracturing of soil to improve remedial actions, Final Report, USEPA 600/2-91-012, NTIS Report PB91-181818, 1991, 298pp.
[3] Shapiro, A.P. and Probstein, R.F., Removal of contaminants from saturated clay by electroosmosis, Environ. Sci. Tech., 27, 1993, 283–287.
[4] Acar, Y.B., Gale, R.J., Putnam, G.A., Hamed, J. and Wong, R.L., Electrochemical processing of soils: theory of pH gradient development by diffusion, migration, and linear convection, J. Environ. Sci. Health, A25(6), 1990, 687–714.
[5] Probstein, R.F. and Hicks, R.E., Removal of contaminants from soils by electric fields, Science, 260, 1993, 498–503.
[6] Runnels, D.D. and Wahli, C., In situ electromigration as a method for removing sulfate, metals and other contaminants from ground water, Ground Water Monitoring Review, 11, 1993, 121.
[7] Lageman, R., Pool, W. and Seffinga, G., Electro-reclamation theory and practice, Chem. Ind. Lond., 18, 1989, 575–579.
[8] Vesper, S.J., Murdoch, L.C., Hayes, S. and Davis-Hoover, W.J., Solid oxygen source for bioremediation in subsurface soils, Journal of Hazardous Materials, 36, 1994, 265–274.
[9] Gillham, R.W. and Burris, D.R., In-situ treatment walls—Chemical dehalogenation, denitrification, and bioaugmentation, Proc. Subsurface Restoration Conf., Dallas, TX, 21–24 June 1992, pp.66–68.
[10] Ho, S.V. and Brodsky, P.H., Integrated in situ technology for soil remediation—the Lasagna process, Proc. Am. Chem. Soc. Annual Meeting, Atlanta, GA, 19–21 Sept. 1994, pp.504–506.
[11] Johnston, I.W. and Butterfield, R., A laboratory investigation of soil consolidation by electro-osmosis, Aust. Geomech. J., 67, 1977, 21–32.
[12] Sundaram, P.N., Hydraulic and electro-osmotic permeability coefficients, J. Geotech. Eng. Div., Proc. ASCE, 105, GT1, 1978, 89–92.
[13] Bear, J., Hydraulics of Groundwater, McGraw-Hill, New York, 1979, 569pp.
[14] Lerch, N.K., Hale, W.F. and Lemaster, D.D., Soil survey of Hamilton County, Ohio, US Department of Agriculture Soil Conservation Service, 1982, 219pp.
[15] Van Genuchten, M.Th., A closed-form equation for predicting the hydraulic conductivity of unsaturated soils, Soil Sci. Soc. Am. J., 44, 1980, 892–898.